CHAPTER

24 Crystallization of G Protein-Coupled Receptors

David Salom*, Pius S. Padayatti*, and Krzysztof Palczewski*,†

*Polgenix Inc., Cleveland, Ohio, USA

†Department of Pharmacology, School of Medicine, Case Western Reserve University, Cleveland, Ohio, USA

CHAPTER OUTLINE

Methods in Cell Biology, Volume 117
ISSN 0091-679X

http://dx.doi.org/10.1016/B978-0-12-408143-7.00024-4

Abstract

Oligomerization is one of several mechanisms that can regulate the activity of G protein-coupled receptors (GPCRs), but little is known about the structure of GPCR oligomers. Crystallography and NMR are the only methods able to reveal the details of receptor–receptor interactions at an atomic level, and several GPCR homodimers already have been described from crystal structures. Two clusters of symmetric interfaces have been identified from these structures that concur with biochemical data, one involving helices I, II, and VIII and the other formed mainly by helices V and VI. In this chapter, we describe the protocols used in our laboratory for the crystallization of rhodopsin and the β2-adrenergic receptor (β2-AR). For bovine rhodopsin, we developed a new purification strategy including a $(NH_4)_2SO_4$-induced phase separation that proved essential to obtain crystals of photoactivated rhodopsin containing parallel dimers. Crystallization of native bovine rhodopsin was achieved by the classic vapor-diffusion technique. For β2-AR, we developed a purification strategy based on previously published protocols employing a lipidic cubic phase to obtain diffracting crystals of a β2-AR/T4-lysozyme chimera bound to the antagonist carazolol.

Abbreviations

CHS	cholesterol hemisuccinate
DDM	dodecyl-β-D-maltoside
FRAP	fluorescence recovery after photobleaching
GPCR	G protein-coupled receptor
LCP	lipidic cubic phase
MES	2-(*N*-morpholino) ethanesulfonic acid
NG	nonyl-β-D-glucoside
ROS	rod outer segment(s)
T4L	T4 lysozyme
β2-AR	β2-adrenergic receptor

INTRODUCTION

After a decade of heated debate, a large body of experimental data now supports the notion that G protein-coupled receptors (GPCRs) can form physiologically relevant oligomers (Milligan, 2008). Therefore, GPCR oligomerization interface(s) are potential targets for allosteric drugs to modulate GPCR function and high-resolution structures of GPCR oligomers are highly sought as templates for structure-based drug design. The first direct structural evidence of GPCR oligomerization was obtained in our laboratory by atomic-force microscopy, showing a paracrystalline arrangement of bovine rhodopsin in native membranes (Fotiadis et al., 2003). Later, parallel rhodopsin dimers were observed in crystals solved by electron crystallography at 5.5 Å (Ruprecht, Mielke, Vogel, Villa, & Schertler, 2004) and by X-ray

crystallography at 3.8 Å (Lodowski et al., 2007; Salom, Le Trong, et al., 2006). Then, a parallel dimer of β2-adrenergic receptor (β2-AR)/T4L was obtained in which the interactions between the two monomers were mainly mediated by lipids (Cherezov et al., 2007). More recently, crystals of chemokine CXCR4 receptor (Wu et al., 2010), κ-opioid receptor (Wu et al., 2012), μ-opioid receptor (Manglik et al., 2012), and β1-AR (Huang, Chen, Zhang, & Huang, 2013) revealed parallel homodimer arrangements with substantial protein–protein interfaces probably reflecting functionally relevant interactions.

24.1 CRYSTALLIZATION OF BOVINE RHODOPSIN

The first crystal structure of ground-state rhodopsin, solved in our laboratory (Palczewski et al., 2000), contained antiparallel dimer interactions and the crystals were disrupted when illuminated. Next, Schertler's laboratory obtained hexagonal rhodopsin crystals (Suda, Filipek, Palczewski, Engel, & Fotiadis, 2004), (Stenkamp, 2008) also with an antiparallel monomer–monomer arrangement. Then, through modifications of rhodopsin's purification protocol, our laboratory obtained two new crystal forms (trigonal and rhombohedral) able to withstand photoactivation. This permitted the structure of an activated GPCR to be solved for the first time (Salom, Le Trong, et al., 2006; Salom, Lodowski, et al., 2006). Interestingly, one of the rhodopsin–rhodopsin interfaces in both crystal forms involving interactions between transmembrane helices I and II and helix VIII is parallel and consistent with the tridimensional model based on the paracrystalline arrangement of rhodopsin observed in native membranes (Fotiadis et al., 2004). In the first part of this chapter, we describe a protocol for the purification and crystallization of rhodopsin in trigonal form, highlighting its most innovative step, the $(NH_4)_2SO_4$-induced phase separation used to concentrate purified rhodopsin prior to crystallization.

24.1.1 Materials

All procedures are performed in a dark room under dim red light at room temperature or colder. The room is equipped with a floor centrifuge, microfuge, spectrophotometer, basic stereo microscope, and 4 °C incubator. Red filters or aluminum foil is used to cover any non-red light from the instruments. This protocol can be scaled down about 10-fold without significant loss in the final rhodopsin yield.

24.1.1.1 Rod outer segment (ROS) isolation with sucrose gradient

1. 100–150 fresh or frozen, dark-adapted, bovine retinas
2. Kuhn's buffer: 67 mM potassium phosphate, pH 7.0, 1 mM $Mg(OAc)_2$, 0.1 mM EDTA (ethylenediaminetetraacetic acid), 1 mM DTT (1,4-dithio-DL-threitol)
3. 45% sucrose in Kuhn's buffer

4. Gradient solutions, with densities to be adjusted with two hydrometers (ranges 1.060–1.130 and 1.120–1.190 g/mL)
   1.10 g/mL (~107 mL of 45% sucrose + 93 mL Kuhn's buffer)
   1.13 g/mL (~167 mL of 45% sucrose + 72 mL Kuhn's buffer)
   1.15 g/mL (~205 mL of 45% sucrose + 41 mL Kuhn's buffer)
5. 40–50 mL high-speed, transparent centrifuge tubes
6. Swinging-bucket rotor able to reach $26{,}500 \times g$
7. 10 mL syringes with luer locks and Popper Laboratory Pipetting Needles, $14G \times 6$ in.
8. Funnel
9. Gauze sponges, 12 ply, 4×4 in.

24.1.1.2 Nonyl-glucoside/$Zn(OAc)_2$ extraction of rhodopsin

1. 0.5 M 2-(*N*-morpholino)ethanesulfonic acid (MES), pH 6.3–6.4
2. 1 M $Zn(OAc)_2$
3. 10% nonyl-β-D-glucoside (NG)
4. UV buffer: 1–5 mM dodecyl-β-D-maltoside (DDM), 50 mM Tris, pH 7.4, 100–150 mM NaCl, and 1 mM hydroxylamine

24.1.1.3 Immunoaffinity purification

1. 1D4 monoclonal antibody coupled to CNBr-activated Sepharose (GE Healthcare Life Sciences) or agarose (Pierce) (90–95 mL of settled gel)
2. Glass column (1–2.5 cm diameter × 20–50 cm length)
3. Peristaltic pump
4. Fraction collector
5. Washing buffer: 25–50 mM NG in 150 mM Tris, pH 7.4, 280 mM NaCl, and 6 mM KCl
6. Elution buffer: 0.5–1 mg/mL TETSQVAPA peptide in washing buffer

24.1.1.4 $(NH_4)_2SO_4$-induced phase separation

1. Solid $(NH_4)_2SO_4$
2. 40–50 mL high-speed, transparent centrifuge tubes
3. Glass rod and small magnetic rod
4. 0.5 M MES, pH 6.3–6.4
5. 2 mL, dolphin-nose bottom, microfuge tubes

24.1.1.5 Crystallization

1. 24-well, greased crystallization plates
2. Transparent microbridges
3. Basic stereo microscope, with 30× and 60× magnification
4. Thick cover slides (0.96 mm × 22 mm × 22 mm)
5. Crystallization buffer: 0–110 mM NG in 50–100 mM MES, pH 6.3–6.4, 12 mM β-mercaptoethanol, 0.1% NaN_3, and 2.5–5% MERPOL HCS
6. Reservoir buffer: 3–3.4 M $(NH_4)_2SO_4$ in 10–50 mM MES, pH 6.3–6.4

24.1.2 Methods

24.1.2.1 ROS isolation with sucrose gradient

The isolation of ROS from dark-adapted bovine retina essentially follows an established sucrose density gradient centrifugation procedure (Papermaster, 1982) with small modifications (Salom, Li, Zhu, Sokal, & Palczewski, 2005). Briefly, shake the retinas for 1 min in 1 volume of 45% sucrose solution and centrifuge for 5 min at $3,300 \times g$. Filter the supernatant through a gauze-lined funnel, dilute it with 1 volume of Kuhn's buffer, and centrifuge for 10 min at $13,000 \times g$. Resuspend the pellet from each tube in 1 mL of 1.10 g/mL sucrose plus 0.5 mL of Kuhn's buffer, and load the suspension into tubes containing a three-step sucrose gradient (10, 16, and 10 mL of densities 1.11, 1.13, and 1.15 g/mL, respectively). After centrifugation for 20 min at $22,000 \times g$, collect the 1.11–1.13 g/mL interface, dilute it with 1 volume of Kuhn's buffer, and recover the ROS by centrifugation at $6,500 \times g$ for 7 min. Store the ROS pellet at −80 °C. Typical recovery is ~0.6 mg rhodopsin per retina.

24.1.2.2 Nonyl-glucoside/$Zn(OAc)_2$ extraction of rhodopsin

Rhodopsin can be selectively extracted from ROS membrane preparations by solubilizing a ROS suspension with alkyl(thio)glucosides in the presence of 2B series divalent cations, which eliminates opsin and other protein contaminants (Okada, Takeda, & Kouyama, 1998).

Resuspend the ROS pellet in ~1 volume of 50 mM MES, pH 6.35. Dissolve a small aliquot in UV buffer and measure its absorbance spectrum from 250 to 700 nm to estimate the rhodopsin concentration ($\varepsilon_{498nm} = 40{,}600\ M^{-1}\ cm^{-1}$; Spalink, Reynolds, Rentzepis, Sperling, & Applebury, 1983). Add the remaining solubilization components from their stock solutions to the ROS suspension to reach final concentrations of 5–10 mg/mL of rhodopsin, 50 mM MES, pH 6.35, 100 mM $Zn(OAc)_2$, and a NG/rhodopsin ratio of 2.2 (w/w). Mix briefly, incubate overnight at 4 °C, and remove precipitated proteins by centrifugation. The A_{280nm}/A_{500nm} ratio of the supernatant typically should be 1.8–2.0, indicating a rhodopsin purity of 80–90%. Up to 50% of rhodopsin can be lost in this step.

24.1.2.3 Immunoaffinity purification of rhodopsin

Preparation of Sepharose-immobilized 1D4 monoclonal antibody is achieved by following the CNBr-activated Sepharose manufacturer's instructions. Antirhodopsin 1D4 antibody can be produced from hybridoma supernatant and purified with a Diethylaminoethyl (DEAE)-cellulose or protein-A column. Alternatively, it can be obtained from mouse ascites fluid and purified with T-Gel (Pierce). We typically coupled the antibody at a ratio of 5 mg of 1D4 per mL of settled gel, resulting in a yield of ~0.5 mg purified rhodopsin per mL of gel.

This is a standard immunoaffinity chromatography step where solubilized ROS (>0.6 mg rhodopsin per mL of settled gel) are slowly loaded onto a prepacked 1D4-Sepharose column (10–20 min), the gel is washed with 5–10 column volumes of washing buffer, and rhodopsin is recovered by addition of 0.5–1 mg/mL of

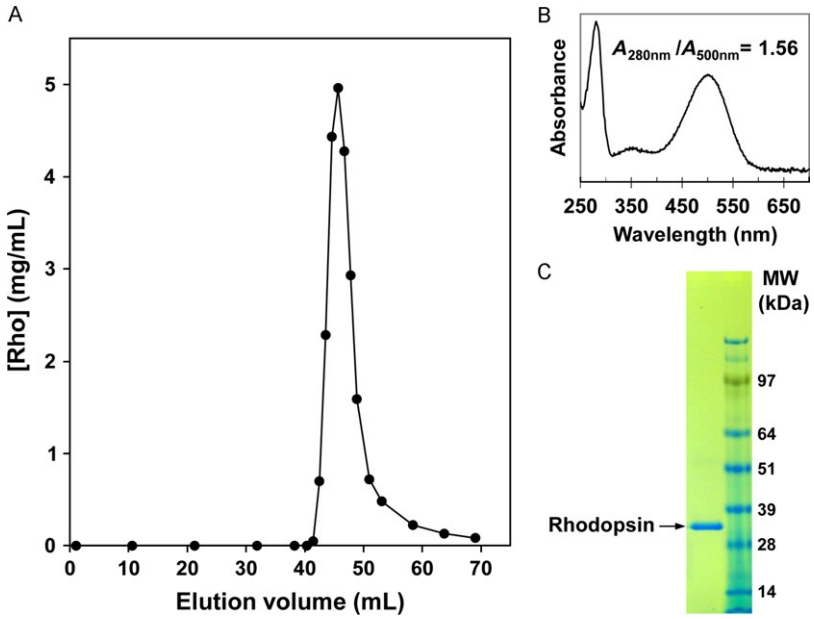

FIGURE 24.1

Immunoaffinity purification of bovine rhodopsin from ROS solubilized in NG. (A) Purified rhodopsin was eluted from a 1.5 cm × 30 cm column containing 46 mL of 1D4-Sepharose. (B) Absorption spectrum of purified rhodopsin (an aliquot was diluted in UV buffer). (C) Coomassie-stained SDS-PAGE gel of purified rhodopsin. MW markers (SeeBlue® Plus2, Invitrogen) are shown in the right lane.

competing peptide. The first fractions with rhodopsin start eluting at ~0.85 column volumes with the peak fraction at ~1.0 column volume (Fig. 24.1A). Elution can be achieved in 1–2 h, but to maximize the peak concentration (up to 6 mg/mL), we typically carried out the elution with 1.5 column volumes of elution buffer for 4 h in a 20–50 cm long column (Salom, Le Trong, et al., 2006). Rhodopsin's purity, assessed by the A_{280nm}/A_{500nm} ratio and electrophoresis, is >99% (Fig. 24.1B and C).

Aliquots of fractions are mixed with UV buffer to measure their rhodopsin absorbance, and those fractions with the highest absorbance are pooled to achieve a rhodopsin concentration of 1–2 mg/mL. Up to 90% of rhodopsin loaded onto the column can be recovered for the next step.

24.1.2.4 $(NH_4)_2SO_4$-induced phase separation

Addition of $(NH_4)_2SO_4$ at saturating concentrations to NG solutions induces a phase separation with a detergent-rich top phase. When rhodopsin purified in NG is treated with $(NH_4)_2SO_4$, the bottom aqueous phase appears completely colorless and rhodopsin can be effectively concentrated up to 25-fold in the top phase (Fig. 24.2A).

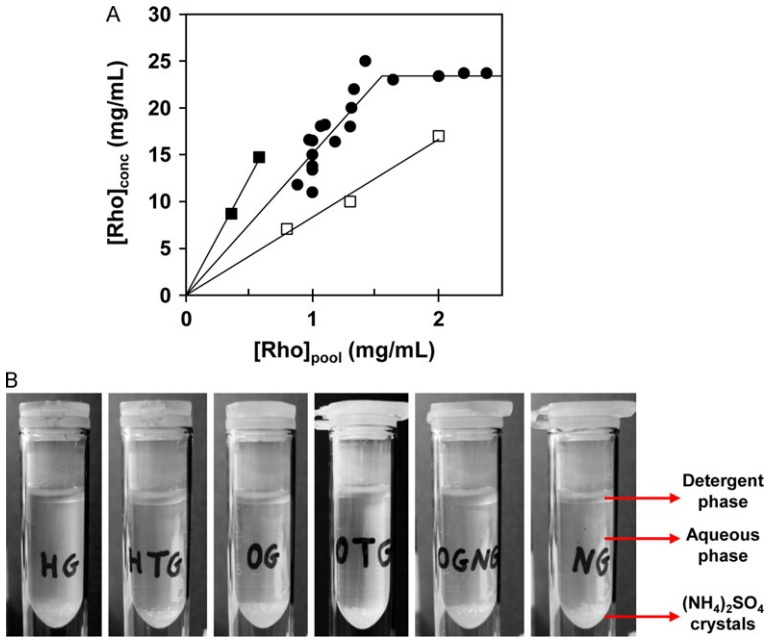

FIGURE 24.2

$(NH_4)_2SO_4$-induced phase separation of purified rhodopsin. (A) Solid $(NH_4)_2SO_4$ was added to rhodopsin purified in 25 mM NG (■), 50 mM NG (•), or 50 mM OG (□). $[Rho]_{pool}$ corresponds to the concentration of rhodopsin prior to treatment with $(NH_4)_2SO_4$, and $[Rho]_{conc}$ is the final concentration of rhodopsin after $(NH_4)_2SO_4$-induced phase separation. Modified and expanded from Salom, Le Trong, et al. (2006). (B) Phase separation in solutions containing 1% detergent in 100 mM MES, pH 6.35, after adding saturating amounts of solid $(NH_4)_2SO_4$ and overnight incubation on ice (HG, heptyl glucoside; HTG, heptyl-thio-glucoside; OG, octyl glucoside; OTG, octyl-thio-glucoside; OGNG, octyl glucoside neopentyl glycol; NG, nonyl glucoside).

- Add 0.25 volumes of 0.5 M MES, pH 6.35, to the pooled purified rhodopsin.
- In a centrifuge tube, weigh ~0.69 g of solid $(NH_4)_2SO_4$ per mL of sample. Take into account that each gram of $(NH_4)_2SO_4$ will add ~0.5 mL to the final volume; therefore, more than one tube could be needed for the entire sample.
- Add the rhodopsin sample to the centrifuge tube(s) (1.45 mL per g of $(NH_4)_2SO_4$, and stir with a small magnetic rod until the solution appears clear (15–30 min). Use a glass rod to assist mixing during the first few minutes until the magnetic rod can stir by itself. Use a tube stand or clamp to keep centrifuge tubes vertical on the magnetic stirrer.
- Incubate the tube(s) on ice for 4–7 days to allow excess $(NH_4)_2SO_4$ to crystallize out of solution. Shorter incubation periods will result in the growth of transparent $(NH_4)_2SO_4$ crystals among the rhodopsin crystals, (Fig. 24.3) thereby complicating

crystallization trials because it can be difficult to distinguish these two crystal forms under red light.
- Spin down briefly at ~13,000 × *g* to compact the detergent/rhodopsin (det/rho) phase.
- With a wide bore 1-mL pipette tip, transfer the top, viscous det/rho phase to microfuge tube(s) (preferably, 2 mL dolphin-nose tubes). Sometimes, the whole det/rho phase holds together and can be transferred to the tube in one move. But often the pipette tip fills up with the $(NH_4)_2SO_4$ phase and just a fraction of the det/rho phase. When the microfuge tubes are full, a brief spin will condense the det/rho phase and the bottom phase can be removed with a gel-loading tip. This process must be repeated several times until all the det/rho phase is transferred to the microfuge tubes and all possible $(NH_4)_2SO_4$ has been removed from underneath. About 70% of the initial rhodopsin is recovered after this step.

Notes: This process is slightly less efficient when rhodopsin is purified in octyl glucoside (OG) (Fig. 24.2A). We tested 16 detergents commonly used for membrane protein purification and found that only alkyl(thio)glucoside detergents could be concentrated to a top, detergent-rich phase with saturated $(NH_4)_2SO_4$ (Fig. 24.2B). Therefore, in principle, any short-chain glucoside detergent could potentially be used to purify membrane proteins prior to their concentration by this $(NH_4)_2SO_4$ treatment.

24.1.2.5 Crystallization

The concentrated rhodopsin sample can be used directly for vapor-diffusion crystallization trials, without mixing with reservoir buffer. However, due to its viscosity, the sample is easier to handle if diluted with ~1 volume of crystallization buffer, another buffered solution, or just water. Different components, concentrations, and volumes of the diluting aqueous solution were tested as crystallization variables and a significant percentage supported crystal growth. A sitting drop over a hanging drop format is preferred. The higher the rhodopsin concentration, the lower the reservoir $(NH_4)_2SO_4$ concentration needed to obtain crystals.

Trigonal rhodopsin crystals can be observed after 1 week of incubation at 4 °C and they grow to full size (>100 μm) in 3–4 weeks. These crystals are very stable and retain their morphology and red color for years when kept at 4 °C in the dark.

For photoactivation, a microbridge containing a drop with several crystals (or a few crystals in mother liquor) should be transferred to a new 24-well plate with reservoir buffer and the well should be sealed. Upon illumination with ~500 nm or white light, crystals quickly turn from red to yellow due to isomerization of 11-*cis*-retinal (a potent antagonist) into all-*trans*-retinal (Fig. 24.3) (rhodopsin cognate agonist). The optimal time from the start of photoactivation until crystal freezing in liquid nitrogen is ~2 h after which diffraction quality slowly deteriorates. If left in a drop, crystal morphology is preserved for weeks or months but eventually crystals turn colorless.

Glucose, sucrose, paraffin oil, and several other cryoprotectants have been used successfully with rhodopsin crystals. Most of the crystals were cryoprotected by adding ~10 μL of ~3 M $(NH_4)_2SO_4$ in 50 mM MES, pH 6.35, to the crystal drops before harvesting. The presence of buffer also slows $(NH_4)_2SO_4$ crystal formation due to evaporation, a benefit especially if multiple rhodopsin crystals are being harvested from the same drop.

Notes: Rhodopsin crystals can be grown without the $(NH_4)_2SO_4$-induced phase separation step, and even without ROS isolation and NG/$Zn(OAc)_2$ extraction. Thus, rhodopsin can be solubilized directly from retinas with NG or DDM and purified with immobilized 1D4. This procedure, if done carefully, produces a sample of rhodopsin at >5 mg/mL that can be used directly for crystallization without a concentration step (Salom, Le Trong, et al., 2006). However, crystals obtained this way diffracted poorly and "melted" upon white light illumination, much like the original tetragonal rhodopsin crystals (Okada et al., 2000). Inclusion of each additional purification step resulted in an increased quality of rhodopsin crystals, and the $(NH_4)_2SO_4$-induced phase separation was essential for obtaining light-stable crystals.

MERPOL DA instead of MERPOL HCS as an additive produced rhombohedral rhodopsin crystals diffracting to 3.8 Å (Salom, Le Trong, et al., 2006). However, these crystals were more difficult to reproduce and, upon illumination, lost diffraction more dramatically than the trigonal crystals. Other additives, especially

FIGURE 24.3

Photoactivated rhodopsin crystals surrounding a colorless $(NH_4)_2SO_4$ crystal.

amphiphiles, had negative and positive effects on crystal and diffraction quality. However, no other crystal form was identified from these crystallization trials.

24.2 CRYSTALLIZATION OF β2-AR

Here, we describe the crystallization in a monoolein/cholesterol lipidic cubic phase (LCP) of a thermostabilized β2-AR(E122W)/T4L construct described in Hanson et al. (Alexandrov, Mileni, Chien, Hanson, & Stevens, 2008; PBD ID 3D4S) as bound to carazolol instead of timolol, with some modifications to the protocol that made crystal growth more reproducible.

The LCP method, first used to crystallize bacteriorhodopsin (Landau & Rosenbusch, 1996), already has been employed to obtain one-tenth of membrane protein structures in the Protein Data Bank (Aherne, Lyons, & Caffrey, 2012) and most structures of engineered GPCRs (Caffrey, Li, & Dukkipati, 2012). Although no strategy was found to favor a particular relative orientation of GPCRs, four of these receptors crystallized in LCP appeared as dimers in a parallel arrangement (β2-AR, CXCR4, and κ- and μ-opioid receptors) (Cherezov & Caffrey, 2007; Chun et al., 2012).

Some of the advantages found with crystallization of GPCRs in mesophase are (i) rapid crystal growth, (ii) mild temperatures used for crystal growth (~20 °C), and (iii) the fact that all crystals obtained so far are type I, formed by stacked layers of two-dimensional crystals that mimic the native membrane. Another strategy to facilitate GPCR crystallization has been to modify their sequences to (i) stabilize the receptors, (ii) remove flexible regions, (iii) enhance their expression, and (iv) increase the receptors' hydrophilic areas. Such sequence modifications include truncation of the third intracellular loop or its substitution by T4L or BRIL (thermostabilized apocytochrome b_{562}), N-terminal fusion of T4L or BRIL, truncation of long N- and C-termini, and/or addition of thermo-stabilizing mutations.

24.2.1 Materials

24.2.1.1 Solubilization of membranes

1. DDM
2. Cholesterol hemisuccinate (CHS)
3. Dounce homogenizer, 100 mL
4. Insect cell (Sf9) pellets expressing the receptor
5. 1 M 4-(2-hydroxyethyl)-1-piperazineethanesulfonic acid (HEPES), pH 7.5
6. 1 M NaCl
7. 1 M $MgCl_2$
8. 1 M KCl
9. Protease inhibitor cocktail, EDTA-free (Roche)
10. Glycopeptide *N*-glycosidase (PNGase F)
11. DNase (for example, Benzonase® nuclease)
12. Iodoacetamide

24.2.1.2 Immunoaffinity and gel filtration chromatography

1. SepSphere TM alprenolol agarose (CellMosaic, LLC, Worcester, MA)
2. Nickel affinity gel (HIS-Select Nickel Affinity Gel, Sigma, St. Louis, MO)
3. Centrifugal concentrators (100 kDa molecular weight cutoff)
4. Gel filtration column—Sepharose 6 10/300 GL column (GE Life Sciences, Piscataway, NJ)
5. Carazolol

24.2.1.3 Crystallization

1. Stock options Salt kit, HR2-245 (Hampton Research, Aliso Viejo, CA)
2. Polyethylene glycol (PEG) 400
3. 1,4-Butanediol
4. HR2-428 additive screen (Hampton Research, Aliso Viejo, CA)
5. Monoolein (Nu-Chek Prep, Inc., Elysian, MN)
6. Cholesterol
7. LCP mixing devices (Emerald Biosystems, Bainbridge Island, WA)
8. LCP sandwich screening plate (Swissci, Hampton Research, Aliso Viejo, CA)
9. Cy3 mono-NHS-reactive dye (GE Life Sciences)

24.2.2 Methods

24.2.2.1 Protein purification

24.2.2.1.1 Crude membrane preparations

Prepare insect cell pellet (from 3 L of cell culture) expressing the β2-AR(E122W)/T4L construct. All following steps should be performed on ice or at 4 °C. The purification of β2-AR is designed to be completed in 2–3 days with an extra day dedicated to crystallization.

Centrifuge the Sf9 cells in phosphate saline buffer (PBS) at 50,000 × *g* for 15 min and homogenize the resulting cell pellet in ~300 mL of minimal buffer (10 mM HEPES, pH 7.5, 1 mM $MgCl_2$, 2 mM KCl and one protease inhibitor tablet per 50 mL) with 20 up and down strokes in a Dounce homogenizer. Centrifuge the resulting homogenate at ~50,000 × *g* for 30 min and discard the supernatant. Repeat the above process at least three times.

Homogenize the combined pellet from the last step into ~400 mL of minimal buffer supplemented with 1 M NaCl and Benzonase. Repeat the membrane washing by centrifugation as in the previous step until a tight pellet is obtained.

24.2.2.1.2 Solubilization

Homogenize the washed membranes in a final volume of 500 mL with solubilization buffer (50 mM HEPES, pH 7.5, 0.15 M NaCl, 1 mM $MgCl_2$, 2 mM KCl, and protease inhibitor cocktail). Then, add PNGase F and more Benzonase. Homogenize with 20 up and down strokes in Dounce homogenizer, add iodoacetamide (2 mg/mL), and incubate at 4 °C for 30–45 min. Add DDM and CHS from a 10 × stock to final concentrations of 0.5% and 0.1%, respectively, and rotate the homogenate for at least 6 h.

24.2.2.1.3 Affinity chromatography

At the end of the incubation, centrifuge the homogenate at 50,000 × *g* for 30 min to remove insoluble material. Add 5 mL of alprenolol-agarose gel to the supernatant and rotate at 4 °C for binding overnight. Next day, recover the alprenolol-agarose gel by pouring it into an empty wide gravitation column and wash the bound protein extensively with washing buffer (150–200 mL of 50 mM HEPES, pH 7.5, 0.15 M NaCl, 0.05% DDM, and 0.01% CHS). Elute the bound receptor batchwise by competition with 2 mM alprenolol in washing buffer (twice with 10 mL and once finally with 5 mL) over a total period of 4–5 h of slow rotation. Check the purity of eluted fractions by SDS-PAGE.

Incubate the eluted protein (25 mL) with ~500 μL of nickel affinity gel and rotate for at least 2 h at 4 °C. Then, wash the nickel affinity gel extensively with 150 mL of washing buffer (50 mM HEPES, pH 7.5, 150 mM NaCl, 0.025% DDM, and 0.005% CHS containing 50 μM carazolol). (This step can also be used for ligand exchange.) Perform elution of the sample at the end of incubation by competition with 1–2 mL of 200 mM imidazole in the washing buffer. Further purify the eluted samples by gel filtration in 50 mM HEPES, pH 7.5, 100 mM NaCl, 0.025% DDM, and 0.005% CHS containing 50 μM carazolol. Concentrate the peak fractions from gel filtration (typically 1–2 mL) up to 50 mg/mL for crystallization. A typical yield from 3 L of culture for the β2-AR is 3–4 mg protein (Fig. 24.4A).

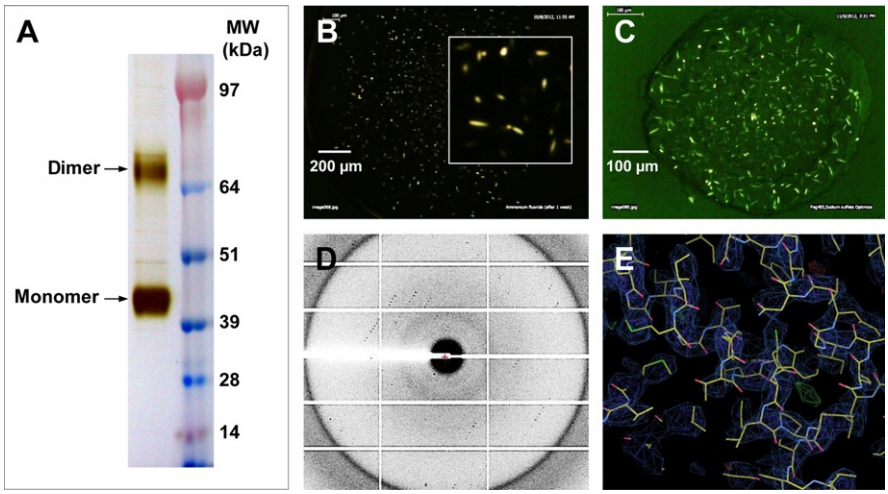

FIGURE 24.4

Crystal structure of β2-AR(E122W)/T4L. (A) SDS-PAGE analysis of a purified β2-AR(E122W)/T4L sample developed with silver staining. Both the purified monomer and dimer are present. (B, C) Representative crystals imaged under crossed polarizers. Inset in panel B shows a close-up of microcrystals. (B) Crystals grown in 0.1 M HEPES, pH 7.0, 0.15 M ammonium fluoride, 30% PEG 400, and 7% 1,4-butanediol. (C) Crystals grown in 0.1 M HEPES, pH 7.0, 0.15 M sodium sulfate, 30% PEG 400, and 7% 1,4-butanediol. (D) Representative X-ray diffraction pattern from a microcrystal with dimensions of 20 × 10 × 5 μm. (E) A part of electron density of β2-AR(E122W)/T4L crystals.

24.2.2.2 Mesophase crystallization

24.2.2.2.1 Preparation of monoolein/cholesterol/protein mixture

To prepare a 10:1 mol/mol monoolein/cholesterol mixture, codissolve appropriate amounts of these lipids in chloroform/methanol (2:1 v/v), evaporate the solvent with a gentle stream of nitrogen, and then keep the dried lipid under high vacuum for at least 6 h. Finally, seal the vials under an argon or nitrogen stream and store them at −20 °C for future use.

Bring the cholesterol-doped monoolein vial up to room temperature for at least an hour. Open the lipid vial and place it at 42 °C until the solid is evenly melted. Clean all syringes thoroughly with methanol first and then water. Then dry out the syringes to remove water before introducing lipids. Melt pure monoolein separately and mix it with doped monoolein if the molar monoolein/cholesterol ratio needs to be higher than 10. With a 200 μL pipette, introduce 50–75 μL of melted lipid/cholesterol mixture through the open end of the syringe with coupler secured at the other end of a 250 μL Hamilton syringe (use of an uneven coupler for LCP mixture (Caffrey & Cherezov, 2009)). Introduce the concentrated protein sample into a 100 μL syringe in a volume sufficient to fully hydrate the lipid (for monoolein at 20 °C, full hydration with water occurs at ∼40% (w/w) water). Typically, if one is using a manual setup, the volume of lipid should be adjusted to ∼22 μL and the volume of protein sample to 14 μL, which will produce enough LCP mixture to set up ∼175 nL of 96 × 2 conditions for manual screening. Both syringes are coupled through an uneven coupler and both solutions are mixed until a clear solution is obtained. Rapid disappearance of the initial turbidity upon mixing indicates a good LCP sample. Overconcentrating the detergent during centrifugal concentration of the sample often results in turbid LCP mixtures. Also, protein concentrations below 10 mg/mL often do not produce crystals. The lipid/protein mixture should appear completely clear and nonbirefringent when a drop is placed between two cover slips and observed under crossed polarizers.

24.2.2.2.2 FRAP assay

To attain buffer and precipitant conditions conducive to diffusion, nucleation, and crystal growth, it is advisable to subject a few micrograms of purified protein to a fluorescence recovery after photobleaching (FRAP) assay (Cherezov, Liu, Griffith, Hanson, & Stevens, 2008). Use a portion of purified material for labeling with Cy3 mono-NHS-reactive dye (as per manufacturer's instructions) and repurify the labeled protein on a gel filtration column to separate the free dye. Use this Cy3-labeled protein, at 1 mg/mL, to analyze the mobility of samples in a FRAP assay by employing a FRAP screen (Xu, Liu, Hanson, Stevens, & Cherezov, 2011).

Initially, a FRAP screen with 48 salts (Stock options Salt kit) combined with PEG 400 concentrations of choice (e.g., 25% in the upper 48 wells and 30% in the lower 48 wells) is set up in a single 96-well plate at pH 7.0. The same plate is then replicated but at two other pHs (e.g., pH 6.0 and 8.0). In addition, several additives can be individually set up to evaluate the effect of each on the protein diffusion rate. Alternatively, one can substitute a different PEG for PEG 400 in FRAP screens. Depending on the outcomes from such FRAP experiments, crystallization

experiments are designed. Typically, only a few salts allow a significant diffusion of the receptor within the mesophase. The faster the diffusion rates for the protein in a set of conditions, the greater the chances of growing crystals under those conditions. For laboratories with no prior mesophase screening experience, we advise undertaking FRAP measurements and LCP setups using β2-AR(E122W)/T4L or human adenosine A_{2a} receptor (PDB ID 4EIY) samples, which reproducibly crystallize without the need of automation.

For a positive control in the diffusion assays, 0.2 M sodium citrate, 28% PEG 400, 0.1 M HEPES, pH 7.5, with carazolol-bound β2-AR can be used, with 0.5 M NaCl employed as a negative control (Xu et al., 2011). Conditions where we observed crystallization of β2-AR (E122W)/T4L that correlate with diffusion rates included one of the following salts: ammonium fluoride, dibasic ammonium phosphate, potassium sulfate, potassium thiocyanate, dibasic sodium phosphate dihydrate, or sodium sulfate. A screen of additives added to the salts in the preceding text (or mixture of salts) and PEG 400 after FRAP assays identified the following compounds as beneficial for the crystallization of β2-AR(E122W)/T4L: ethylene glycol, 1,6-hexanediol, 1,3-butanediol, 2-propanol, 1,4-butanediol, tert-butanol, 1,3-propanediol, and 1-propanol.

The first crystal hits obtained from initial screens are generally not suitable for X-ray diffraction. Thus, individual conditions should be expanded by extensive fine grid screens around the initial conditions. Some initial hits, despite such fine screening, did not improve, although the use of ammonium fluoride, ammonium phosphate, and sodium sulfate along with 28–30% PEG 400 and 1,4-butanediol (5–8%) produced diffraction quality crystals of a $20 \times 10 \times 5$ μm size (Fig. 24.4B and C). The most important variable in growing larger crystals is the monoolein/cholesterol ratio (cholesterol was varied from 3 to 10 mol%). Usually, adding cholesterol to monoolein slowed crystal growth from 2 days to 2 weeks.

24.2.2.2.3 Monitoring crystal growth

A detailed observation record should be kept for every crystallization tray, no matter how small the changes observed. Excellent guidelines were established by pioneers in the field (Caffrey & Cherezov, 2009). An automated plate reader is a good investment because, as in any crystallization trial, once one starts setting drops, the number of trials grows exponentially. Many setups show crystal growth over a month but plates beyond a month tend to dry out. This can be delayed by assuring that the sandwich tape has no trapped bubbles, wrapping the plates with aluminum foil, and incubating them at 22 °C.

A crossed polarizer-fitted microscope with good quality optics is all one needs to monitor the crystallization process from mesophase setups (Fig. 24.4B and C). However, other more expensive imaging options are recommended to discriminate between salt and protein crystals and avoid wasting valuable time and resources following false leads. For example, microscopes equipped with UV fluorescence (Judge, Swift, & Gonzalez, 2005), Second-order nonlinear optical imaging of chiral crystals (SONICC) (Kissick, Gualtieri, Simpson, & Cherezov, 2010), two-photon excited UV fluorescence (Madden, Dewalt, & Simpson, 2011), or two-photon excited

visible fluorescence combined with second harmonic generation (Padayatti, Palczewska, Sun, Palczewski, & Salom, 2012) can help in this regard.

The first breakthrough in any mesophase crystallization trial is obtaining the initial microcrystals, no matter how small or insignificant they may appear. The next follow-up steps are to reproducibly grow microcrystals followed by optimization to obtain larger crystals. Crystal sizes as small as $10 \times 5 \times 2$ μm are adequate for X-ray diffraction data collection at modern beamlines equipped with microfocus and rastering capabilities (we used beamlines 23-ID (GMC-A) and 24-ID (NE-CAT) at APS, Argonne, IL). Moreover, the promise of free-electron laser techniques in collecting data from protein nanocrystals holds great hope for the future (Dilanian, Streltsov, Quiney, & Nugent, 2013; Kang, Lee, & Drew, 2013).

We collected a full data set from a single β2-AR(E122W)/T4L crystal. X-ray diffraction data are shown in Fig. 24.4D, with spots extending down to 3.4 Å. The resulting molecular replacement solution, along with the corresponding electron density map, is shown in Fig. 24.4E.

24.3 DISCUSSION

We have described two very different strategies for GPCR crystallization that can be adapted to the crystallization of other GPCRs.

Rhodopsin, being a stable and abundant receptor, can be obtained from native sources and most of the experimental procedures can be performed at room temperature. Trigonal crystals grow very reproducibly in a classic vapor-diffusion format. The most challenging requirement is the need to work in a dark room under dim red light.

After the crystal structure of rhodopsin was initially solved, it took 7 years to solve the structure of the first GPCR with a diffusible ligand, β2-AR/T4L (Cherezov et al., 2007). This was enabled mainly by advances in protein engineering, crystallization methods, and X-ray collection, which allowed solving the structures of at least 17 more GPCRs in the following 6 years. In addition, sequence modifications engineered into the β2-AR to enhance its crystallization can also be used as a reference, although they are often not directly transferable to other GPCRs. Therefore, before attempting the crystallization of a novel GPCR target, we recommend that multiple protein constructs be subjected to several "stress tests" (thermostability assays, expression level assays, homogeneity determination by gel filtration, purification yields, radioligand binding, FRAP assays, etc.) before the three to four best constructs are selected for crystallization trials.

Acknowledgments

The X-ray diffraction data were collected at 24-ID-C (NE-CAT) beamline at APS, Chicago. The authors thank Wenyu Sun for help with insect cell cultures and Philip Kiser for diffraction data collection.

References

Aherne, M., Lyons, J. A., & Caffrey, M. (2012). A fast, simple and robust protocol for growing crystals in the lipidic cubic phase. *Journal of Applied Crystallography*, *45*(Pt 6), 1330–1333.

Alexandrov, A. I., Mileni, M., Chien, E. Y., Hanson, M. A., & Stevens, R. C. (2008). Microscale fluorescent thermal stability assay for membrane proteins. *Structure*, *16*(3), 351–359.

Caffrey, M., & Cherezov, V. (2009). Crystallizing membrane proteins using lipidic mesophases. *Nature Protocols*, *4*(5), 706–731.

Caffrey, M., Li, D., & Dukkipati, A. (2012). Membrane protein structure determination using crystallography and lipidic mesophases: Recent advances and successes. *Biochemistry*, *51*(32), 6266–6288.

Cherezov, V., & Caffrey, M. (2007). Membrane protein crystallization in lipidic mesophases. A mechanism study using X-ray microdiffraction. *Faraday Discussions*, *136*, 195–212, discussion 213–129.

Cherezov, V., Liu, J., Griffith, M., Hanson, M. A., & Stevens, R. C. (2008). LCP-FRAP assay for pre-screening membrane proteins for in meso crystallization. *Crystal Growth & Design*, *8*(12), 4307–4315.

Cherezov, V., Rosenbaum, D. M., Hanson, M. A., Rasmussen, S. G., Thian, F. S., Kobilka, T. S., et al. (2007). High-resolution crystal structure of an engineered human beta2-adrenergic G protein-coupled receptor. *Science*, *318*(5854), 1258–1265.

Chun, E., Thompson, A. A., Liu, W., Roth, C. B., Griffith, M. T., Katritch, V., et al. (2012). Fusion partner toolchest for the stabilization and crystallization of g protein-coupled receptors. *Structure*, *20*(6), 967–976.

Dilanian, R. A., Streltsov, V. A., Quiney, H. M., & Nugent, K. A. (2013). Continuous X-ray diffractive field in protein nanocrystallography. *Acta Crystallographica. Section A*, *69*(Pt 1), 108–118.

Fotiadis, D., Liang, Y., Filipek, S., Saperstein, D. A., Engel, A., & Palczewski, K. (2003). Atomic-force microscopy: Rhodopsin dimers in native disc membranes. *Nature*, *421*(6919), 127–128.

Fotiadis, D., Liang, Y., Filipek, S., Saperstein, D. A., Engel, A., & Palczewski, K. (2004). The G protein-coupled receptor rhodopsin in the native membrane. *FEBS Letters*, *564*(3), 281–288.

Huang, J., Chen, S., Zhang, J. J., & Huang, X. Y. (2013). Crystal structure of oligomeric β1-adrenergic G protein-coupled receptors in ligand-free basal state. *Nature Structural and Molecular Biology*, *20*(4), 419–425.

Judge, R. A., Swift, K., & Gonzalez, C. (2005). An ultraviolet fluorescence-based method for identifying and distinguishing protein crystals. *Acta Crystallographica, Section D: Biological Crystallography*, *61*(Pt 1), 60–66.

Kang, H. J., Lee, C., & Drew, D. (2013). Breaking the barriers in membrane protein crystallography. *International Journal of Biochemistry & Cell Biology*, *45*(3), 636–644.

Kissick, D. J., Gualtieri, E. J., Simpson, G. J., & Cherezov, V. (2010). Nonlinear optical imaging of integral membrane protein crystals in lipidic mesophases. *Analytical Chemistry*, *82*(2), 491–497.

Landau, E. M., & Rosenbusch, J. P. (1996). Lipidic cubic phases: A novel concept for the crystallization of membrane proteins. *Proceedings of the National Academy of Sciences of the United States of America*, *93*(25), 14532–14535.

Lodowski, D. T., Salom, D., Le Trong, I., Teller, D. C., Ballesteros, J. A., Palczewski, K., et al. (2007). Crystal packing analysis of Rhodopsin crystals. *Journal of Structural Biology*, *158*(3), 455–462.

Madden, J. T., Dewalt, E. L., & Simpson, G. J. (2011). Two-photon excited UV fluorescence for protein crystal detection. *Acta Crystallographica, Section D: Biological Crystallography*, *67*(Pt 10), 839–846.

Manglik, A., Kruse, A. C., Kobilka, T. S., Thian, F. S., Mathiesen, J. M., Sunahara, R. K., et al. (2012). Crystal structure of the μ-opioid receptor bound to a morphinan antagonist. *Nature*, *485*(7398), 321–326.

Milligan, G. (2008). A day in the life of a G protein-coupled receptor: The contribution to function of G protein-coupled receptor dimerization. *British Journal of Pharmacology*, *153*(Suppl. 1), S216–S229.

Okada, T., Le Trong, I., Fox, B. A., Behnke, C. A., Stenkamp, R. E., & Palczewski, K. (2000). X-ray diffraction analysis of three-dimensional crystals of bovine rhodopsin obtained from mixed micelles. *Journal of Structural Biology*, *130*(1), 73–80.

Okada, T., Takeda, K., & Kouyama, T. (1998). Highly selective separation of rhodopsin from bovine rod outer segment membranes using combination of divalent cation and alkyl(thio) glucoside. *Photochemistry and Photobiology*, *67*(5), 495–499.

Padayatti, P., Palczewska, G., Sun, W., Palczewski, K., & Salom, D. (2012). Imaging of protein crystals with two-photon microscopy. *Biochemistry*, *51*(8), 1625–1637.

Palczewski, K., Kumasaka, T., Hori, T., Behnke, C. A., Motoshima, H., Fox, B. A., et al. (2000). Crystal structure of rhodopsin: A G protein-coupled receptor. *Science*, *289*(5480), 739–745.

Papermaster, D. S. (1982). Preparation of retinal rod outer segments. *Methods in Enzymology*, *81*, 48–52.

Ruprecht, J. J., Mielke, T., Vogel, R., Villa, C., & Schertler, G. F. (2004). Electron crystallography reveals the structure of metarhodopsin I. *EMBO Journal*, *23*(18), 3609–3620.

Salom, D., Le Trong, I., Pohl, E., Ballesteros, J. A., Stenkamp, R. E., Palczewski, K., et al. (2006). Improvements in G protein-coupled receptor purification yield light stable rhodopsin crystals. *Journal of Structural Biology*, *156*(3), 497–504.

Salom, D., Li, N., Zhu, L., Sokal, I., & Palczewski, K. (2005). Purification of the G protein-coupled receptor rhodopsin for structural studies. In S. R. George & B. F. O'Dowd (Eds.), *G protein-coupled receptor–protein interactions* (pp. 1–17). Hoboken: John Wiley & Sons, Inc.

Salom, D., Lodowski, D. T., Stenkamp, R. E., Le Trong, I., Golczak, M., Jastrzebska, B., et al. (2006). Crystal structure of a photoactivated deprotonated intermediate of rhodopsin. *Proceedings of the National Academy of Sciences of the United States of America*, *103*(44), 16123–16128.

Spalink, J. D., Reynolds, A. H., Rentzepis, P. M., Sperling, W., & Applebury, M. L. (1983). Bathorhodopsin intermediates from 11-cis-rhodopsin and 9-cis-rhodopsin. *Proceedings of the National Academy of Sciences of the United States of America*, *80*(7), 1887–1891.

Stenkamp, R. E. (2008). Alternative models for two crystal structures of bovine rhodopsin. *Acta Crystallographica, Section D: Biological Crystallography*, *D64*(Pt 8), 902–904.

Suda, K., Filipek, S., Palczewski, K., Engel, A., & Fotiadis, D. (2004). The supramolecular structure of the GPCR rhodopsin in solution and native disc membranes. *Molecular Membrane Biology*, *21*(6), 435–446.

Wu, B., Chien, E. Y., Mol, C. D., Fenalti, G., Liu, W., Katritch, V., et al. (2010). Structures of the CXCR4 chemokine GPCR with small-molecule and cyclic peptide antagonists. *Science*, *330*(6007), 1066–1071.

Wu, H., Wacker, D., Mileni, M., Katritch, V., Han, G. W., Vardy, E., et al. (2012). Structure of the human kappa-opioid receptor in complex with JDTic. *Nature*, *485*(7398), 327–332.

Xu, F., Liu, W., Hanson, M. A., Stevens, R. C., & Cherezov, V. (2011). Development of an automated high throughput LCP-FRAP assay to guide membrane protein crystallization in lipid mesophases. *Crystal Growth & Design*, *11*(4), 1193–1201.